Food & Function

PAPER

Cite this: *Food Funct.*, 2019, **10**, 1816

Targeted delivery of phycocyanin for the prevention of colon cancer using electrospun fibers†

Peng Wen,‡[a] Teng-Gen Hu,‡[a,b] Yan Wen,[a] Robert J. Linhardt,[c] Min-Hua Zong,[a] Yu-Xiao Zou[a,b] and Hong Wu*[a]

Received 11th December 2018,
Accepted 10th February 2019

DOI: 10.1039/c8fo02447b

rsc.li/food-function

Phycocyanin (PC), a water-soluble biliprotein, exhibits potent anti-colon cancer properties. However, its application in functional foods is limited by the poor stability and low bioavailability of PC. In this study, we successfully encapsulated PC by coaxial electrospinning. The colon targeted release of PC was achieved with retention of the antioxidant activity of PC. The PC-loaded electrospun fiber mat (EFM) obtained inhibited HCT116 cell growth in a dose-dependent and time-dependent manner. In particular, the PC-loaded EFM exerted its anti-cancer activity by blocking the cell cycle at the G_0/G_1 phase and inducing cell apoptosis involving the decrease of Bcl-2/Bax, activation of caspase 3 and release of cytochrome c. This study suggests that co-axial electrospinning is an efficient and effective way to deliver PC and improve its bioavailability; thus, it represents a promising approach for encapsulating functional ingredients for colon cancer prevention.

Introduction

Extensive studies have demonstrated that many bioactive compounds, isolated or purified from food or food supplements, possess health-promoting effects.[1] In this regard, phycocyanin (PC), a nutraceutical compound derived from seaweed, exhibits strong anti-inflammatory, anti-oxidant, and radical scavenging activities.[2,3] Many studies have documented that PC selectively exerts a therapeutic effect on cancer cells, while it has little or no toxic side effect on normal cells.[4,5] In particular, the crucial inhibitory effect of PC on colon cancer, a common worldwide health threat, has been shown. Thangam *et al.* discovered that PC could significantly inhibit the growth of HT29 cells;[6] Lu *et al.* reported that PC induced the apoptosis of colon carcinoma COLO 205 cells through the mitochondrial pathway.[7] Unfortunately, the stability and bioavailability of PC are unsuited for oral administration due to significant barriers when passing through the upper gastrointestinal tract (GIT),[8] thus limiting its potential applications in the fields of functional foods and pharmaceuticals. Moreover, the anti-colon cancer activity of ingested PC remains unclear. Therefore, exploring an effective delivery approach for PC that maintains its anti-colon cancer activity is necessary.

An oral colon-specific controlled release system appears to be an ideal delivery system, since it has been demonstrated to be a promising approach for achieving colon targeting or for treating colon disease.[9] Based on the physiological character of the colon, various strategies have been proposed for the fabrication of a colon targeting system, and a microflora-activated system exhibits greater site-specificity compared to pH-dependent and time-dependent systems.[10,11] Natural polysaccharide-based polymers, such as chitosan (CS), guar gum, sodium alginate (SA), resistant starch, *etc.*, have received tremendous attention since they exhibit promising potential for their use as microflora-activated colon-targeting systems. Studies have shown that the use of a combination of polysaccharides would be more effective for achieving targeted delivery compared to the use of a single polysaccharide.[12,13]

Recently, the potential of a nanotechnology-based delivery system has been widely recognized and it is regarded as a valuable tool to fill the gaps left by conventional oral delivery systems.[14,15] In particular, nano-encapsulation has emerged as one of the most interesting approaches in the pharmaceutical and food industries, and nano-systems can be applied as carriers of functional compounds, aimed at targeted delivery, con-

[a]*School of Food Science and Engineering, Guangdong Province Key Laboratory for Green Processing of Natural Products and Product Safety, South China University of Technology, Guangzhou 510640, China. E-mail: bbhwu@scut.edu.cn*
[b]*Sericultural & Agri-Food Research Institute, Guangdong Academy of Agricultural Sciences; Key Laboratory of Functional Foods, Ministry of Agriculture, Guangdong Key Laboratory of Agricultural Products Processing, China*
[c]*Department of Chemical and Biological Engineering, Center for Biotechnology and Interdisciplinary Studies, Rensselaer Polytechnic Institute, Troy, New York 12180, USA*

† Electronic supplementary information (ESI) available. See DOI: 10.1039/c8fo02447b

‡ These authors have contributed equally and are co-first authors.

trolled release or preserving their activity during food processing and/or oral ingestion.[16] Among these approaches, electrospinning, a simple, mild and cost-effective technology, has attracted great attention for the encapsulation of bioactive compounds. Furthermore, the electrospun fibers can serve as a versatile novel delivery vehicle.[16–19] In our recent work, the encapsulation of hydrophobic quercetin and a model protein by polysaccharide-based electrospun fibers was achieved and its colon-specific performance was confirmed.[20,21] However, the feasibility of this delivery system on bioactive protein has not yet been verified. In particular, there is very limited information on the anti-cancer activity of an ingested PC-loaded electrospun fiber mat on HCT116 colon cancer cells and its underlying mechanism of action studies.

Accordingly, in this study, a colonic PC-loaded delivery system based on both solubility dependent on pH and specific bacterial enzymatic erosion was constructed by coaxial electrospinning to maximize the pharmacological properties of PC on HCT116 cells. The release profile of PC and the inhibition against HCT116 cells were evaluated, as well as the probable molecular mechanism related to the induction of apoptosis in HCT116 cells.

Materials and methods

Materials

PC with a purity ratio (A_{620}/A_{280}) of 1.79 was purchased from Taizhou Binmei Biotechnology Co., Ltd (Taizhou, China); CS (160 kDa, DD was 87%) was purchased from Dacheng Biotech. Co. Ltd (Weifang, China). β-Glucosidase, SA (viscosity 15–25 cps) and tripolyphosphate (TPP) were obtained from Sigma-Aldrich (Shanghai, China). 1,1-Diphenyl-2-picrylhydrazyl (DPPH) was provided by Shanghai Yuanye Bio-Technology Co. Ltd (Shanghai, China). Polyoxyethylene (PEO), trypsin and pepsin were from Aladdin Biological Technology Co., Ltd (Shanghai, China). Fetal bovine serum (FBS), penicillin/streptomycin, and Dulbecco's modified Eagle's medium (DMEM) were purchased from Gibco Life Technologies, Paisley, UK. Propidium iodide (PI), FluoroPure grade dihydrochloride (DAPI), a BCA protein assay kit and an annexin V-FITC/PI apoptosis detection kit, RNase, and skimmed milk were purchased from Beyotime Biotechnology Co. Ltd (Shanghai, China). Antibodies were purchased from Cell Signaling Technology (Danvers, MA, USA). Polyvinyl alcohol (PVA) was purchased from Tianma Fine Chemical Factory (Guangzhou, China). CCC-HIE-2 cells were obtained from Guangdong Academy of Agricultural Sciences (Guangzhou, China). HCT116 cells were purchased from the Cell Library of the Chinese Academy of Sciences (Shanghai, China). All other chemicals used were of analytical grade.

Preparation and characterization of PC-loaded CS nanoparticles (PCNPs)

First, based on preliminary tests, PCNPs were prepared by the ionic-gelation method. A TPP solution (1 mg mL^{-1}) was added to the CS (3 mg mL^{-1}, dissolved in 1% acetic acid, pH 5.3) solution that had been previously mixed with a PC (1.5 mg mL^{-1}) solution to achieve the mass ratio of 5 : 1 for CS : TPP. The PCNPs spontaneously formed and were recovered by centrifugation at 18 000 rpm for 15 min at 10 °C. The encapsulation efficiency (EE) of PC in PCNPs was investigated according to the method described by Castangia *et al.*[22] Transmission electron microscopy (TEM, JEOL, Japan) was applied to determine PCNP size. The stability of the QCNP was evaluated by measuring the average size and ζ-potential over a period of 30 days at 4 °C and 25 °C by dynamic light scattering (DLS) using a Zetasizer nano-ZS (Malvern Instruments, Worcestershire, UK). The antioxidant activity of PCNPs was investigated using the DPPH radical-scavenging assay.

Optimization of the electrospinning process

The PC-loaded EFM was then prepared by co-axial electrospinning. The composition of the electrospinning solution was as follows: a PCNP suspension, as obtained above, and PVA (10% w/w) in a volume ratio of 2 : 1 comprised the core layer, while the shell layer was composed of SA and PEO (total polymer 9%, 80 : 20, w/w) solution that was prepared in water/ethanol (90 : 10, v/v). The response surface methodology (RSM) was employed to optimize the electrospinning process based on preliminary tests. The levels for response surface design are shown in Table S1.† A scanning electron microscope (SEM, Zeiss EVO 18, Carl Zeiss, Jena, Germany) and a transmission electron microscope (TEM, JEOL, Japan) were used to observe the nanofiber morphology.[23]

In vitro release study

The release behavior of PC from PC-loaded EFM was investigated using the method of Wen *et al.*[24] At predetermined times, 2 mL of a release medium was collected and replaced by adding an equal volume of fresh medium. The PC content was calculated, and the release data of PC were then fitted using different models:

$$\text{Higuchi}: \frac{M_t}{M_\infty} = kt^{1/2} \quad (1)$$

$$\text{Ritger--Peppas}: \frac{M_t}{M_\infty} = kt^n \quad (2)$$

The antioxidant activity of the released PC was also studied.

Cell growth and morphology in nanofibers

The HCT116 cells were cultured in DMEM supplemented with 10% FBS, penicillin (50 IU mL^{-1}) and streptomycin (50 IU mL^{-1}). The cells were kept at 37 °C in a 5% CO_2 incubator, and the medium was changed every two days. The biocompatibility of the obtained PC-loaded EFM matrix was evaluated by observing the behavior of normal human intestinal CCC-HIE-2 cells cultured on the crosslinked fiber mat as described previously.[25] The optical density (OD) was measured using a microplate reader and viable cells on the EFM were also

observed by SEM to study the cell proliferation capacity on EFM.

The effect of PC-loaded EFM on HCT116 colon cancer cells was measured by the CCK-8 assay. First, different amounts of PC-loaded EFM were immersed in digestive fluids (simulated gastric fluid (SGF) for 2 h, simulated intestinal fluid (SIF) for 4 h, and simulated colon fluid (SCF) for 14 h) to obtain the released PC. 100 μL of cell suspension were placed into 96-well plates (10^4 cells per well), after incubation for 24 h, they were treated with different concentrations of the released PC. Cells incubated without released PC were maintained as a control. After incubation for different times, the cell viability was determined by the CCK-8 assay according to the manufacturer's instructions. The IC_{50} (the inhibitory concentration required for 50% reduction of the cell number) value was obtained. After treatment with the released PC for the indicated time, the cells were harvested, stained with PI for 10 min in the dark, and visualized using a fluorescence microscope.

Cell cycle and apoptosis analysis

HCT116 cells (2×10^5 cells per well) were placed into 24-well tissue culture plates. After 24 h, the cells were treated with the released PC medium for 48 h. In the cell cycle study, the harvested cells were fixed in 80% (v/v) ethanol at 4 °C for 2 h, and then washed with PBS. The collected cells were re-suspended in cold PBS containing and PI, Triton X-100 and RNase A for 20 min in the dark. The cell cycle distribution was analyzed using flow cytometry. The apoptotic cells were determined using the Annexin V/PI kit. Briefly, the treated cells were detached, harvested and re-suspend into in annexin V-FITC and PI labelling solution for 15 min (10^6 cells per mL) before analysis using flow cytometry.

Western blot analysis

HCT116 cells were cultured for 48 h at 37 °C in 6-well plates in the presence of different concentrations of PC release medium. After washing with PBS, the cells were lysed and the protein concentration was determined using a Bradford assay. Proteins (30 μg per lane) were separated using sodium dodecyl sulfate-polyacrylamide gels (SDS-PAGE), and then electro-transferred to PVDF membranes. Afterwards, the membranes were blocked in a TBS–Tween 20 (0.1%, v/v) solution containing 5% (w/v) non-fat milk for 2 h, followed by overnight incubation with primary antibodies at 4 °C for 14 h. After being washed with TBS-Tween 20 buffer, the membranes were incubated with the secondary antibody (horseradish peroxidase) for 1 h, followed by detection using enhanced chemiluminescence reagents. The optical densities of the bands were analyzed using ImageJ software.

Statistical analysis

All data are presented as the mean ± standard deviation (SD). Statistical analysis was performed using analysis of variance (ANOVA) and the Duncan *t*-test. Differences were considered significant at $P \leq 0.05$.

Results and discussion

Preparation and characterization of PC-loaded EFM

At first, the PCNPs were prepared and their TEM image revealed that a single PCNP had a spherical structure and the average particle size was 53.2 nm (Fig. 1a). Studies have confirmed that PC possesses antioxidant activity.[26,27] In this study, the DPPH radical-scavenging method was employed to determine the antioxidant activity of the encapsulated PC. DPPH is a steady nitrogen-based free radical and the color can change from violet to yellow when it reacts with proton-donating compounds. Fig. 1b clearly shows that PCNP could scavenge DPPH radicals in a dose-dependent manner, and the DC50 of PCNP was reached at a concentration of 452 μg mL^{-1}. This trend is the same as that observed by Chentir *et al.*[28] In line with this study, PC with a purity ratio of 1.39 exhibited a DPPH radical scavenging activity of 60% at 0.4 mg mL^{-1}.[29] Thus, we conclude that PC had been effectively encapsulated into the NP. The stability of the PCNP was next assessed by measuring the particle size, ζ-potential and EE under different storage conditions (4 °C and 25 °C). After 1 month storage, the mean particle size of PCNP ranged from 260.6 nm to 274.7 nm and from 258.3 nm to 290.8 nm when stored at 4 °C and 25 °C, respectively. Similarly, the ζ-potential varied from 31.6 mV to 30.3 mV and 31.4 mV to 28.1 mV for 4 °C and 25 °C, respectively. There was no apparent change in the particle size or charge (Table 1). In contrast, the EE of the PCNP decreased by about 4.3% and 10.5% after 1 month storage at 4 °C and 25 °C, respectively. This reduction might be caused by the oxidation of PC molecules. Therefore, it can be concluded that storage at 4 °C was favorable to maintain PCNP's stability.

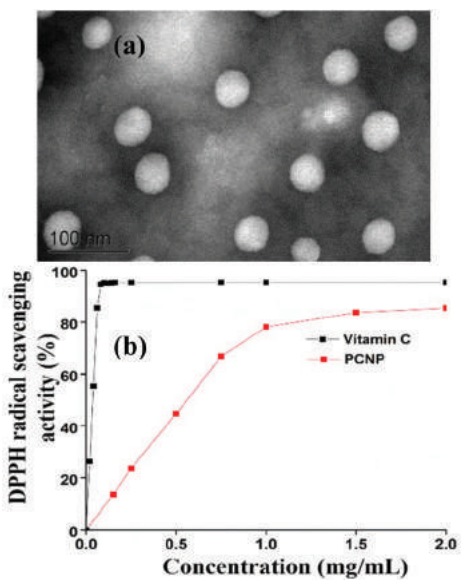

Fig. 1 (a) TEM image and (b) antioxidant activity of PCNP.

Table 1 Physical characterization and antioxidant activity of PCNP after 1 month of storage

	PCNP	Average size (nm)	ζ-Potential (mV)	EE (%)
4 °C	Fresh	260.6 ± 1.9	31.6 ± 1.1	82.1 ± 0.2
	1 months	274.7 ± 1.5	30.3 ± 1.4	78.6 ± 0.3
25 °C	Fresh	258.3 ± 1.6	31.4 ± 1.0	81.8 ± 0.3
	1 months	290.8 ± 2.2	28.1 ± 1.8	73.2 ± 0.4

Optimization of the electrospinning process

Then, the core-sheath PC-loaded EFM was fabricated using PCNP and PVA as the core layer and SA and PEO as the shell layer. During electrospinning, some process parameters are known to influence the morphology of EFM.[30,31] As shown in Fig. 2, an increase in electrospinning distance from 13 cm to 15 cm can reduce the beaded-fibers and form thin fibers. Similarly, a low voltage is favorable for producing fibers of uniform morphology (<20 kV). Higher feed rates (≥0.45 mL h^{-1}) can result in fibers with a wide distribution of diameters. However, the conventional approach of examining single factor experiments does not take into account the combined effects of multiple electrospinning parameters. Based on the results of our preliminary tests (Fig. 2), RSM was employed to investigate the interaction among different parameters and optimize multiple factors to obtain uniform, beaded-free fibers (Table S2†). The average fiber diameter was chosen as the response, and the 3D surface plots and contours of the models are depicted in Fig. 3. On increasing the applied voltage, the fiber diameter was affected in different ways depending on the electrospinning distance selected. This is because the electrospinning distance has a significant effect on the jet flight time and electric field strength. At low voltages, the flight time is the dominant factor. Longer spinning distance leads to more time for jet stretching, thus generating thinner fibers. However, when the voltage is high, the solution can be drawn very quickly to the collector, which results in the

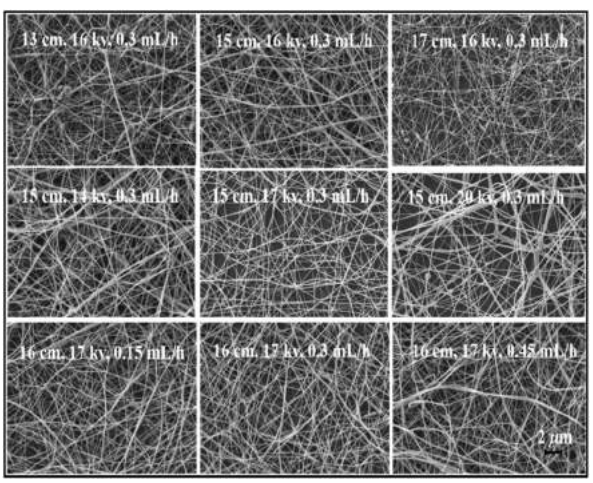

Fig. 2 Representative SEM images of the effect of different electrospinning parameters on the fiber morphology.

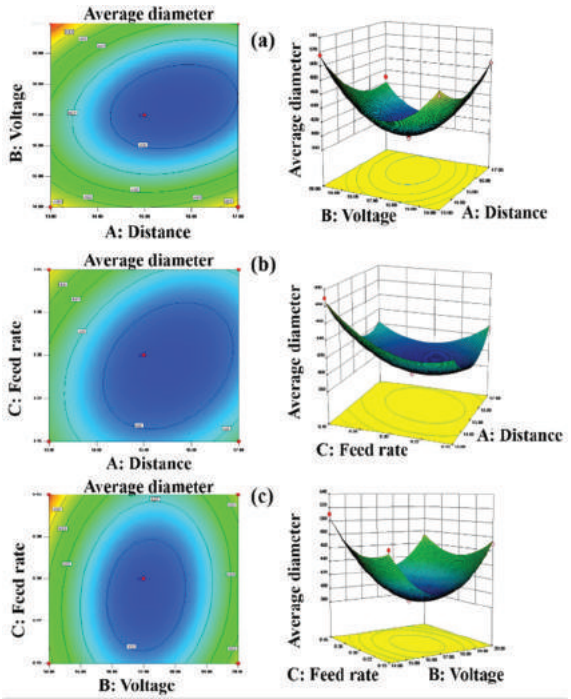

Fig. 3 Response surfaces for the average diameter in terms of (a) voltage and distance, (b) distance and feed rate, and (c) feed rate and voltage.

increase of fiber diameter. Hence, the balance between the voltage and the distance determines the final fiber diameter. In addition, the effect of the feed rate on the fiber diameter and distribution also needs to be assessed. A minimum value for the feed rate is required to maintain a stable Taylor cone. The effect of the feed rate can be the determining factor for fiber diameter at long electrospinning distances or when the electric field strength is low. The ANOVA results revealed that all parameters significantly impact the fiber diameter ($P < 0.05$) (Table S3†). The *R*-squared value obtained was 0.9907, indicating that the model is very consistent with the experimentally obtained results. The quality of the estimated residuals in a straight line and the data in the model was good since they were scattered randomly in the residual *versus* predicted plot (Fig. S1†). The optimized parameters were: voltage = 17.23 kV, distance = 15.57 cm and feed rate = 0.29 mL h^{-1}, and the fitted equation was:

$$\begin{aligned}\text{Average diameter} = {} & 402.21332 - 20.03146 \times \text{Distance} - 23.99386 \\ & \times \text{Voltage} + 64.58500 \times \text{Feed rate} - 0.38458 \\ & \times \text{Distance} \times \text{Voltage} - 6.26667 \times \text{Distance} \\ & \times \text{Feed rate} - 2.81667 \times \text{Voltage} \times \text{Feed rate} \\ & + 0.91350 \times \text{Distance}^2 + 0.89294 \times \text{Voltage}^2 \\ & + 142.62222 \times \text{Feed rate}^2.\end{aligned}$$

As shown in Fig. S2,† the obtained fibers exhibit a core–sheath structure with the core layer being 220 nm and the sheath layer being 350 nm (Fig. S2†).

Colon targeted release behavior of PC

The PC-loaded EFM was placed in the simulated digestion fluids to investigate the PC release profile. The PC-loaded EFM with an average diameter of 390 nm showed that only a small amount of PC (around 3%) was released in simulated gastric fluid (SGF) due to the resistance of SA to the acidic environment (Fig. 4). In the simulated intestinal fluid (SIF) for 4 h, about 14% PC was released and the core component of CS retarded the further swelling of EFM that could promote the release of more PC. After immersion in simulated colonic fluid (SCF) for 14 h, the EFM showed that approximately 74% PC was released due to the degradation of the CS carrier through the action of β-glucosidase. Thus, the colon-specific release behavior of PC from the EFM was demonstrated. In addition, it has been reported that the electrospun fibers were more favorable for the release of encapsulated compounds than are cast films.[32,33] In the current study, the amount of released PC increased with the decrease of fiber diameter. In particular, for SCF, approximately 5.5% h^{-1} and 5.1% h^{-1} of PC were released from fibers of diameters 410 nm and 740 nm, respectively. We believe that this is related to the specific surface area of the fiber; the thinner the fiber diameter, the larger the fiber surface area. Hence, faster release of PC is achieved using EFM having a small fiber diameter. This release behavior is similar to that reported by Wang *et al.*[34]

In addition to the colon targeting release behavior, the antioxidant activity of the released PC after *in vitro* digestion was also evaluated using the DPPH method. The DPPH scavenging rate (%) for free PC (equivalent amount of encapsulated PC in the EFM) was 82.2% (data not shown). As shown in Fig. 4, after the gastric (2 h) and intestinal digestion (4 h), the scavenging rates of the released PC were approximately 4.8% and 13.5%, respectively, for fibers having a diameter of 410 nm. This was because a small amount of PC was released as demonstrated in the above release profile. In SCF, the scavenging rates of the released PC were about 64.9%, suggesting that the activity of the released PC was maintained. Moreover, with an increase in fiber diameter (740 nm), lower antioxidant activity was detected, as the rates were 3.6%, 11.2% and 60.8%

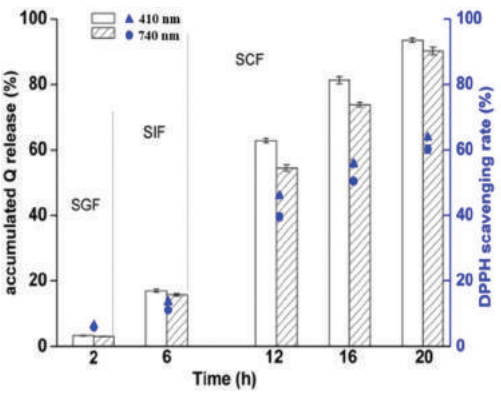

Fig. 4 Release profile and antioxidant activity of PC from PC-loaded EFM with different average diameters under simulated digestive fluids.

for SGF, SIF and SCF, respectively. This phenomenon is also consistent with the PC release study (above) showing decreased release with increasing average fiber diameter. These data demonstrate the protective effect of electrospun fibers on the antioxidant activity of PC as well as the colon-specific release behavior.

The release mechanism of PC from fibers under different pH conditions was studied by fitting the release data of PC to different equations. The Higuchi model describes a release mechanism based on Fickian diffusion, while the Ritger–Peppas model indicates that more than one type of release mechanism may be involved, and the release exponent n was calculated according to the first 60% release amount. As shown in Table 2, higher R^2 values were achieved for the Higuchi model in SGF and SIF, suggesting that the PC release followed a Fickian diffusion mechanism. In SCF, the PC release data were more in line with the Ritger–Peppas model ($R^2 > 0.99$). The n value suggests that the PC release involves a super Case II transport mechanism, in which the degradation of the polymer matrix was dominant.[35] Hence, the model supports the conclusion that the release of PC from EFM in SCF took place as a result of the erosion of CS.

Biocompatibility study

The biocompatibility of PC-loaded EFM on normal intestinal CCC-HIE-2 cells was characterized *in vitro* according to ISO 10993-5 standards.[36] After incubation for 24, 72, and 120 h, the OD values were determined as these reflect the number of viable cells on the EFM (Fig. 5a). Although the absorbance intensity was lower than the absorbance of the control, the absorbance ratio still reached 80% of the negative control value, demonstrating that the PC-loaded EFM had no significant cytotoxicity towards CCC-HIE-2 cells. SEM was also employed to investigate the proliferation of CCC-HIE-2 cells on the EFM surface (Fig. 5b–d). At 24 h, small amounts of cells were seen on the EFM surface; after incubation for 72 h, the CCC-HIE-2 cells integrated well with the surrounding fibers and exhibited intercellular tight junctions with adjacent cells. At 120 h, a continuous monolayer covering the PC-loaded EFM surface was observed, indicating good interaction between cells and fibers. These results suggest that the PC-loaded EFM had good biocompatibility with normal intestinal cells; hence, it could be potentially exploited as a good candidate carrier for drug delivery.

Effect of PC-loaded EFM on cell proliferation

PC has been reported to be an effective agent against colon cancer. The effect of PC-loaded EFM on colon cancer HCT116 cells was next determined using a CCK-8 assay. After treatment of HCT116 cells with PC-loaded EFM, the percentage inhibition of cancer cell proliferation was determined. The cytotoxicity of PC-EFM was found to be dose dependent (Fig. 6). Cell viability also decreased with the increase of the incubation time. The calculated IC_{50} values were 24.17, 19.43 and 12.82 mg mL^{-1} (the corresponding PC concentrations were 371.73, 298.83 and 197.17 μg mL^{-1}) after 24 h, 48 h and 72 h

Table 2 Fitting results with different release kinetics in different media

	Model	Equation	(r^2)	Release kinetics data	Transport mechanism
SGF	Higuchi	$Q = 0.03157t^{1/2} - 0.02011$	0.98577	$k_H = 0.03157$	**Fickian diffusion**
	Ritger–Peppas	$\log Q = 1.05037 \log t - 0.05766$	0.95203		
SIF	Higuchi	$Q = 0.11566t^{1/2} - 0.07169$	0.99825	$k_H = 0.11566$	**Fickian diffusion**
	Ritger–Peppas	$\log Q = 0.93457 \log t + 0.59622$	0.97413		
SCF	Higuchi	$Q = 0.21358t^{1/2} - 0.2005421$	0.96869		
	Ritger–Peppas	$\log Q = 0.94523 \log t + 0.71195$	0.99827	$n = 0.94523$	**Super Case II transport**

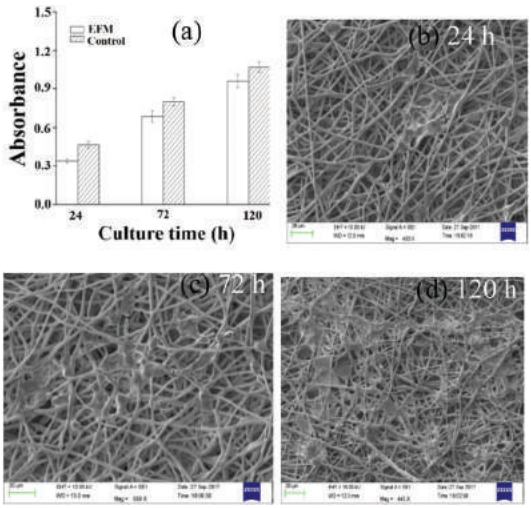

Fig. 5 The biocompatibility of PC-loaded nEFM on CCC-HIE-2 cells: (a) the OD values of cultured cells and (b, c, d) representative SEM images of cells cultured for different times on EFM.

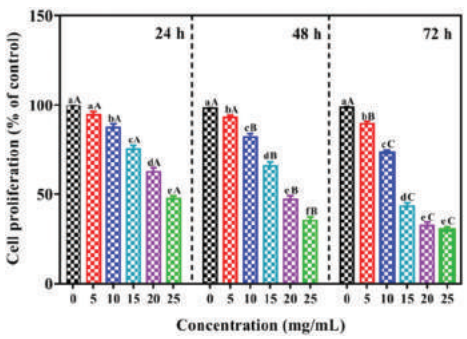

Fig. 6 Effect of different concentrations of PC-loaded EFM on HCT116 cell proliferation at different times. The significance of the analysis was determined. Concentrations within the same treatment time not sharing the same lowercase letters are significantly different ($p < 0.05$). Different capital letters indicate a significant difference ($p < 0.05$) among different incubation times at a specific concentration.

of HCT116 cell incubation, respectively. The resulting data clearly indicated that the growth of HCT116 cells was inhibited by PC-loaded EFM in a dose-dependent and time-dependent manner. This trend is consistent with a previous research study carried out in MDA-MB-231 cells.[37] Jiang *et al.* also reported that the IC_{50} values of PC were 229.0 μg ml^{-1} and 189.4 μg ml^{-1} after 24 h and 48 h treatment of breast cancer MDA-MB-231 cells.[38] Another study pointed out that the recombinant α-subunit of C-phycocyanin (CpcA) induced the death of human colon carcinoma COLO 205 cells up to 46%, using CpcA at 5 μM over 72 h.[7] The different anti-proliferation activity may be related to the purity of PC and the type of cancer cell.

The inhibitory effect of the PC-loaded EFM on HCT116 cells was also investigated by fluorescence microscopy (Fig. 7). Untreated HCT116 cells showed a weak blue fluorescence, indicating an even distribution of chromatin in the nucleolus. After treatment with different concentrations of PC-loaded EFM for specific time, the cell's fraction of condensed contents also presented a dose- and time-dependent manner. Furthermore, a high PC concentration caused a significant reduction in cell viability using fluorescence microscopy, which is consistent with the results of the CCK-8 assay, indicating a PC cancer prevention effect and a pro-apoptotic effect on HCT116 cells.

Cell cycle analysis and western blot analysis of related proteins

Since PC inhibited the proliferation of HCT116 cells, we further explored the effects of PC-loaded EFM on cell cycle progress. There are three major checkpoints for the cell cycle; these include the G_0/G_1, S and G_2/M phase detection points. Previous studies have shown that PC can affect cancer cell cycle progression.[38] In this study, the effect of PC-loaded EFM on cell cycle was also evaluated by flow cytometry and representative histograms for the cell cycle distribution in HCT116

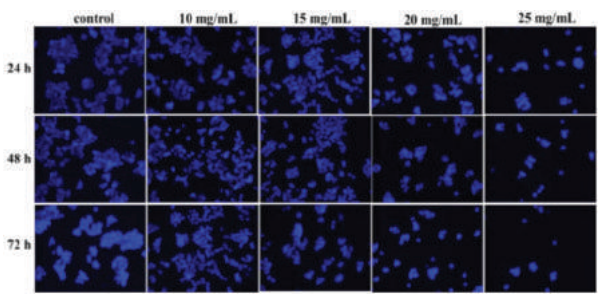

Fig. 7 Fluorescence microscopy of HCT116 cells treated with PC-loaded EFM.

cells are shown in Fig. 8a. Treatment of HCT116 cells with PC-loaded EFM for 48 h resulted in an increase of the G_0/G_1 phase compared with the control. The G_1 phase increased from 53.8% in the control to 65.7% and finally changed to 73.0% after treatment with 15 mg mL^{-1} and 25 mg mL^{-1} PC-loaded EFM, respectively. This increase was coupled with a decreased percentage in S and G_2/M phases. Correspondingly, the S peak decreased from 28.2% in the control to 20.4% and then to 16.7%. These results indicate that PC-loaded EFM induces G_0/G_1 phase cell cycle arrest in HCT116 cells.

This may be because PC acts as a G_1 checkpoint that blocks the progress in the S phase and prevents the replication of DNA.[39] A similar result was found in colon cancer HT29 cells.[6]

It has been reported that cell cycle progression is partly regulated by a family of protein kinase complexes, cyclin-dependent kinases (CDKs) and their activating partners, the cyclins.[40,41] During the G_0/G_1 phase progression, cyclin D1 binds to CDK4/CDK6, resulting in the formation of the cyclin D1/CDK4 complex, eventually driving the cell from G_1 to S phase. However, CDK inhibitors (CDKIs), like p21 and p27, can suppress CDK activity by forming CDK–CDKI complexes.[42] The current study reveals that PC treatment caused a marked reduction of cyclin D1 and CDK4 in a dose-dependent manner, while an increase in the expression level of p21 is also observed (Fig. 8b). Hence, the results indicate that the cell cycle arrest at G_0/G_1 phase of PC is due to the inhibition of cyclin D1 and CDK4 and the up-regulation of p21 expression in HCT116 cells.

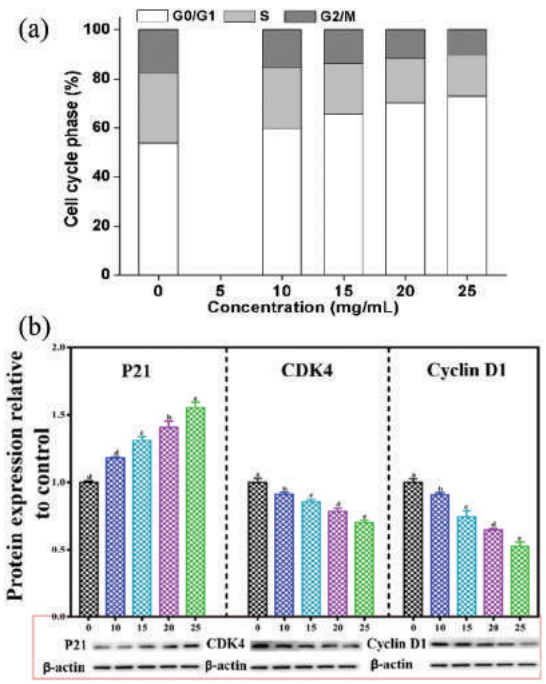

Fig. 8 (a) Effect of various concentrations of PC-loaded EFM on HCT116 cell cycle distribution; (b) cell-cycle regulatory proteins in the HCT116 cells after treatment with PC-loaded EFM for 48 h, as determined by western blot analysis.

Detection of apoptotic cells and western blot analysis of apoptosis-related proteins

HCT116 cancer cells were treated with PC-loaded EFM followed by staining with annexin V/PI to evaluate whether PC-loaded EFM could induce apoptosis. PC induced early apoptosis (annexin V^+/PI^-) and late apoptosis (annexin V^+/PI^+) in a dose-dependent manner in HCT116 cells (Fig. 9). The percentage of early apoptotic cells increased gradually from 16.9% to 22.5% and 42.7% with the increase of PC-loaded EFM concentration from 10 mg mL^{-1} to 20 mg mL^{-1}. Consistent with these results, the percentage of late apoptotic cells increased gradually from 2.9% to 4.7% and 6.7% in treated cells. It can be seen that HCT116 cells are sensitive to PC-loaded EFM induced apoptosis.

We next evaluated the expression of the apoptosis related proteins to clarify the mechanism underlying the apoptosis caused by PC in the HCT116 cells treated. β-Actin was used as the control to ensure the equal loading of proteins in all samples. There are two major apoptotic pathways as the mechanism of apoptosis: one is the mitochondrial/cytochrome C (endogenous) pathway, which is regulated by various members of the Bcl-2 family; the other one is the cell membrane surface death receptor (exogenous) pathway.[4] Usually, different proteins of the Bcl-2 family associated with controlling mitochondrial permeability and cytochrome c expression have been implicated in triggering or preventing apoptosis. Among these, Bcl-2 is a 28 kDa anti-apoptotic protein, which inhibits ROS production, cytochrome c release, and caspase-3 activation, and Bax is a 23 kDa protein that functions as an agonist of apoptosis, facilitating cytochrome C release, and triggering caspase-mediated apoptotic cell death. Hence, the Bcl-2/Bax ratio represents the degree of apoptosis. Researchers have found that PC is capable of activating the mitochondrial/cytochrome C (endogenous) pathway, altering the Bcl-2/Bax

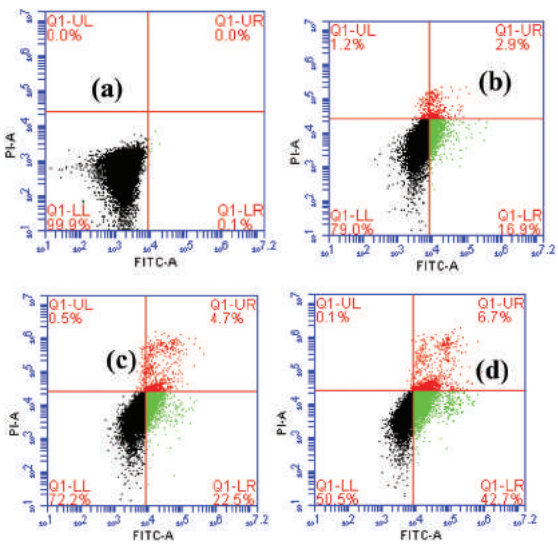

Fig. 9 Effects of different concentrations of PC-loaded EFM (a – 0 mg mL^{-1}, b – 10 mg mL^{-1}, c – 15 mg mL^{-1}, d – 20 mg mL^{-1}) on HCT116 cell apoptosis.

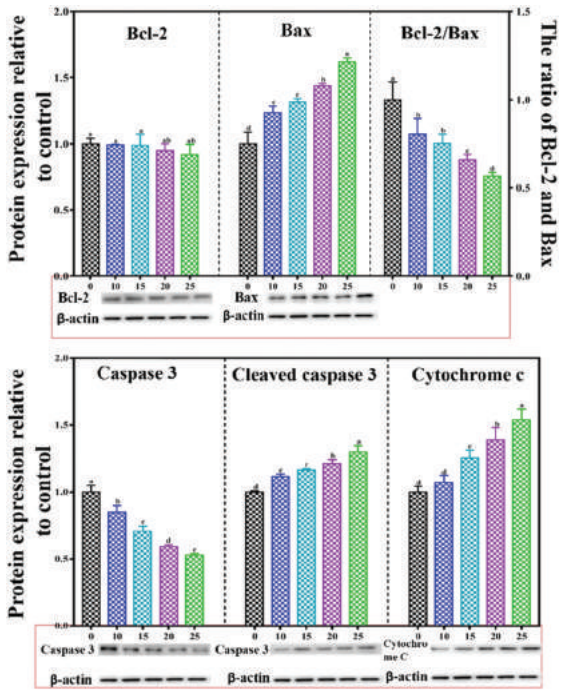

Fig. 10 Western blot analysis of the relative expressions of Bcl-2, Bax, Bcl-2/Bax ratio, caspase-3, C caspase-3 (cleaved caspase-3) and cytochrome C. Analysis of significance was carried out. Different letters indicate a significant difference ($p < 0.05$).

ratio and activating caspases on the apoptosis of MBA-MD-231 cells and HepG2 cells.[37,43] However, the molecular mechanisms of PC-induced apoptosis in HCT116 cells remain unclear. As is shown, the expression of Bax was up-regulated in a dose-dependent manner; however, the Bcl-2 protein levels were almost unchanged (Fig. 10). Even so, the expression ratio of Bcl-2/Bax was apparently decreased in favor of apoptosis. The reduction of Bcl-2/Bax may be related with the loss of mitochondrial membrane potential and the release of cytochrome *c*. As expected, cytochrome *c* in the cytosol of PC-loaded EFM treated cells was observed, and it also increased in a dose-dependent manner. This phenomenon demonstrates an involvement of the mitochondrial pathway in PC-loaded EFM-induced apoptosis. PC-loaded EFM treatment results in a decrease in the pro-caspase 3 level (32 kDa, the precursor form of caspase-3) and simultaneously an increase in the expression of the cleaved form of caspase 3 (Fig. 10), suggesting the activation of caspase 3, which leads to the cleavage of cellular substrates and eventually causes apoptosis. These results indicate that the anti-proliferative activity of PC-loaded EFM on hct116 cells is mediated through apoptosis involving an increase of Bax/Bcl2, activation of caspase 3 and release of cytochrome *c*.

Conclusions

An effective colon targeting system for the controlled release of PC was developed by co-axial electrospinning. The core-sheath structured EFM containing PC exhibited a uniform and bead-free morphology by optimizing the electrospinning parameters using RSM. Owing to the protective effect of electrospun fibers, the antioxidant activity of the released PC after *in vitro* digestion was also observed, as well as colon-specific release properties. PC-loaded EFM inhibited HCT116 cell proliferation through cell cycle arrest at the G_0/G_1 phase and induction of apoptosis. The most probable apoptosis mechanism involved is the one that was mediated by the mitochondrial pathway, which is relevant for stimulating the activity of caspase-3, decreasing the rate of Bcl-2/Bax and the release of cytochrome c. This delivery system could be potentially exploited as a good candidate for the targeted and sustained delivery of bioprotein/peptides to the colon for the prevention of colon cancer. However, the detailed mechanism is still not completely clarified in the current study, and further investigation of PC-loaded EFM in a mouse model is necessary to explore its activity toward cancer cells *in vivo*.

Conflicts of interest

There are no conflicts to declare.

Acknowledgements

We acknowledge the Natural Science Foundation of Guangdong Province (No.2017A030313148), the National Natural Science Foundation of China (No. 31671852), the Science and Technology Project of Guangzhou City (No. 201804010151), the Open Project Program of Provincial Key Laboratory of Green Processing Technology and Product Safety of Natural Products (KL-2018-02) and the Applied Research & Development Special Foundation of Guangdong Province (No. 2015B020234006) for financial support.

References

1 D. J. McClements, *et al.*, Structural Design Principles for Delivery of Bioactive Components in Nutraceuticals and Functional Foods, *Crit. Rev. Food Sci. Nutr.*, 2009, **49**(6), 577–606.
2 P. Yu, *et al.*, Purification and bioactivities of phycocyanin, *Crit. Rev. Food Sci. Nutr.*, 2017, **57**(18), 3840–3849.
3 B. Fernández-Rojas, J. Hernández-Juárez and J. Pedraza-Chaverri, Nutraceutical properties of phycocyanin, *J. Funct. Foods*, 2014, **11**, 375–392.
4 L. Jiang, *et al.*, Phycocyanin: A Potential Drug for Cancer Treatment, *J. Cancer*, 2017, **8**(17), 3416–3429.
5 S. Hao, *et al.*, The In Vitro Anti-Tumor Activity of Phycocyanin against Non-Small Cell Lung Cancer Cells, *Mar. Drugs*, 2018, **16**(6), 178.
6 R. Thangam, *et al.*, C-Phycocyanin from Oscillatoria tenuis exhibited an antioxidant and in vitro antiproliferative

activity through induction of apoptosis and G0/G1 cell cycle arrest, *Food Chem.*, 2013, **140**(1), 262–272.
7 W. Lu, P. Yu and J. Li, Induction of apoptosis in human colon carcinoma COLO 205 cells by the recombinant α subunit of C-phycocyanin, *Biotechnol. Lett.*, 2011, **33**(3), 637–644.
8 P. Yang, *et al.*, Carboxymethyl chitosan nanoparticles coupled with CD59-specific ligand peptide for targeted delivery of C-phycocyanin to HeLa cells, *Tumor Biol.*, 2017, **39**(3), 1010428317692267.
9 W. Situ, *et al.*, Resistant Starch Film-Coated Microparticles for an Oral Colon-Specific Polypeptide Delivery System and Its Release Behaviors, *J. Agric. Food Chem.*, 2014, **62**(16), 3599–3609.
10 S. Sharma and V. R. Sinha, Current pharmaceutical strategies for efficient site specific delivery in inflamed distal intestinal mucosa, *J. Controlled Release*, 2018, **272**, 97–106.
11 M. M. Patel and A. F. Amin, Recent Trends in Microbially and/or Enzymatically Driven Colon-Specific Drug Delivery Systems, *Crit. Rev. Ther. Drug Carrier Syst.*, 2011, **28**(6), 489–552.
12 T. Cerchiara, *et al.*, Microparticles based on chitosan/carboxymethylcellulose polyelectrolyte complexes for colon delivery of vancomycin, *Carbohydr. Polym.*, 2016, **143**, 124–130.
13 C. Caddeo, *et al.*, Chitosan-xanthan gum microparticle-based oral tablet for colon-targeted and sustained delivery of quercetin, *J. Microencapsulation*, 2014, **31**(7), 694–699.
14 P. Parhi, C. Mohanty and S. K. Sahoo, Nanotechnology-based combinational drug delivery: an emerging approach for cancer therapy, *Drug Discovery Today*, 2012, **17**(17–18), 1044–1052.
15 G. Calixto, *et al.*, Nanotechnology-based drug delivery systems for treatment of oral cancer: a review, *Int. J. Nanomed.*, 2014, **9**, 3719–3735.
16 P. N. Ezhilarasi, *et al.*, Nanoencapsulation Techniques for Food Bioactive Components: A Review, *Food Bioprocess Technol.*, 2013, **6**(3), 628–647.
17 H. Wang, *et al.*, Kinetics and Antioxidant Capacity of Proanthocyanidins Encapsulated in Zein Electrospun Fibers by Cyclic Voltammetry, *J. Agric. Food Chem.*, 2016, **64**(15), 3083–3090.
18 B. Ghorani and N. Tucker, Fundamentals of electrospinning as a novel delivery vehicle for bioactive compounds in food nanotechnology, *Food Hydrocolloids*, 2015, **51**, 227–240.
19 X. L. Hu, *et al.*, Electrospinning of polymeric nanofibers for drug delivery applications, *J. Controlled Release*, 2014, **185**, 12–21.
20 P. Wen, *et al.*, Electrospun core-shell structured nanofilm as a novel colon-specific delivery system for protein, *Carbohydr. Polym.*, 2017, **169**, 157–166.
21 P. Wen, *et al.*, Preparation and Characterization of Electrospun Colon-Specific Delivery System for Quercetin and Its Antiproliferative Effect on Cancer Cells, *J. Agric. Food Chem.*, 2018, **66**(44), 11550–11559.
22 I. Castangia, *et al.*, Phycocyanin-encapsulating hyalurosomes as carrier for skin delivery and protection from oxidative stress damage, *J. Mater. Sci.: Mater. Med.*, 2016, **27**(4), 75.
23 P. Wen, *et al.*, Electrospun core-shell structured nanofilm as a novel colon-specific delivery system for protein, *Carbohydr. Polym.*, 2017, **169**, 157–166.
24 P. Wen, *et al.*, Preparation and Characterization of Protein-Loaded Electrospun Fiber Mat and Its Release Kinetics, *J. Agric. Food Chem.*, 2017, **65**(23), 4786–4796.
25 P. Wen, *et al.*, Preparation and Characterization of Electrospun Colon-Specific Delivery System for Quercetin and Its Antiproliferative Effect on Cancer Cells, *J. Agric. Food Chem.*, 2018, **66**(44), 11550–11559.
26 M. Suzery, *et al.*, *Improvement of Stability and Antioxidant Activities by Using Phycocyanin-Chitosan Encapsulation Technique*, in *IOP Conference Series: Earth and Environmental Science*, IOP Publishing, 2017.
27 Z. Huang, *et al.*, Characterization and antioxidant activity of selenium-containing phycocyanin isolated from Spirulina platensis, *Food Chem.*, 2007, **100**(3), 1137–1143.
28 I. Chentir, *et al.*, Stability, bio-functionality and bio-activity of crude phycocyanin from a two-phase cultured Saharian Arthrospira sp strain, *Algal Res.*, 2018, **35**, 395–406.
29 X. Chen, *et al.*, Preparation, characterization of food grade phycobiliproteins from Porphyra haitanensis and the application in liposome-meat system, *LWT – Food Sci. Technol.*, 2017, **77**, 468–474.
30 N. Okutan, P. Terzi and F. Altay, Affecting parameters on electrospinning process and characterization of electrospun gelatin nanofibers, *Food Hydrocolloids*, 2014, **39**, 19–26.
31 C. Drosou, M. Krokida and C. G. Biliaderis, Composite pullulan-whey protein nanofibers made by electrospinning: Impact of process parameters on fiber morphology and physical properties, *Food Hydrocolloids*, 2018, **77**, 726–735.
32 L. Deng, *et al.*, Characterization of gelatin/zein films fabricated by electrospinning vs solvent casting, *Food Hydrocolloids*, 2018, **74**, 324–332.
33 P. Wen, *et al.*, Fabrication of electrospun polylactic acid nanofilm incorporating cinnamon essential oil/beta-cyclodextrin inclusion complex for antimicrobial packaging, *Food Chem.*, 2016, **196**, 996–1004.
34 M. Wang, L. Wang and Y. Huang, Electrospun hydroxypropyl methyl cellulose phthalate (HPMCM/Erythromycin fibers for targeted release in intestine, *J. Appl. Polym. Sci.*, 2007, **106**(4), 2177–2184.
35 X. Wang, *et al.*, Electrospun medicated shellac nanofibers for colon-targeted drug delivery, *Int. J. Pharm.*, 2015, **490**(1), 384–390.
36 Y. Sun, *et al.* Assessment of the biocompatibility of photosensitive polyimide for implantable medical device use, *J. Biomed. Mater. Res., Part A*, 2009, **90A**(3), 648–655.
37 S. Bharathiraja, *et al.*, In Vitro Photodynamic Effect of Phycocyanin against Breast Cancer Cells, *Molecules*, 2016, **21**(11), 1470.

38 L. Jiang, *et al.*, C-Phycocyanin exerts anti-cancer effects via the MAPK signaling pathway in MDA-MB-231 cells, *Cancer Cell Int.*, 2018, **18**(1), 12.
39 K. Vermeulen, Z. N. Berneman and D. R. Van Bockstaele, Cell cycle and apoptosis, *Cell Proliferation*, 2003, **36**(3), 165–175.
40 D. J. Lew and S. Kornbluth, Regulatory roles of cyclin dependent kinase phosphorylation in cell cycle control, *Curr. Opin. Cell Biol.*, 1996, **8**(6), 795–804.
41 J. L. Walker and R. K. Assoian, Integrin-dependent signal transduction regulating cyclin D1 expression and G1 phase cell cycle progression, *Cancer Metastasis Rev.*, 2005, **24**(3), 383–393.
42 C. J. Sherr and J. M. Roberts, CDK inhibitors: positive and negative regulators of G1-phase progression, *Genes Dev.*, 1999, **13**(12), 1501–1512.
43 K. R. Roy, *et al.*, Alteration of mitochondrial membrane potential by Spirulina platensis C-phycocyanin induces apoptosis in the doxorubicinresistant human hepatocellular-carcinoma cell line HepG2, *Biotechnol. Appl. Biochem.*, 2007, **47**(3), 159–167.